Lab on a Chip

PAPER

View Article Online
View Journal | View Issue

Cite this: *Lab Chip*, 2025, **25**, 6324

Multiplexed detection of respiratory viral pathogens by isothermal amplification on an autonomously loaded chip at the point-of-care

Beatrise Berzina, †[ab] Krishna Gupta, †[ab] Rayan Suliman,[cde] Peter Mirtschink,[d] Alexander Dalpke, [cf] Carsten Werner, [ab] Elisha Krieg *[ab] and Lars David Renner *[a]

Recent viral outbreaks have shown the need for reliable diagnostic platforms to rapidly detect various viral and bacterial pathogens at the point-of-care. Over the last decade, isothermal nucleic acid amplification methods have emerged as an appealing alternative to standardized polymerase chain reaction (PCR) tests due to their high sensitivity, selectivity, low cost, and simple assay setup. Virtually all nucleic acid testing platforms require a labor-intensive sample preparation step, limiting the scalability and usability of recent alternatives. This article describes multiplexed isothermal detection of respiratory viruses on a valve-free, autonomously loading microfluidic platform—*VirChip*. We demonstrate that an optimized loop-mediated isothermal amplification (LAMP) enables the simultaneous detection of SARS-CoV-2, influenza A, influenza B, and RSV (A/B) with a limit of detection of 100 RNA copies per reaction. The platform is highly selective, as no cross-reactivity amongst the targeted pathogens was observed in patient samples. Furthermore, crude nasal swab samples can be directly applied to the chip, eliminating the requirement for expensive and laborious RNA isolation and sample workup. *VirChip* facilitates rapid, inexpensive, and multiplexed detection, allowing pathogen screening by primary care providers not only in hospitals but also in resource-limited areas.

Received 23rd May 2025,
Accepted 26th September 2025

DOI: 10.1039/d5lc00509d

rsc.li/loc

Introduction

The coronavirus pandemic has demonstrated a critical need to improve the ability to control infectious disease outbreaks by rapidly identifying and isolating contagious individuals in various settings. This challenge so far requires well-equipped testing facilities with highly trained personnel. However, diagnostic testing in such facilities is expensive and time-consuming, and often not available in resource-limited areas. The recent global spreading of H5N1 ("bird flu") and the possible transmission to humans further underlines these concerns.[1]

Whereas rapid antigen detection has seen tremendous development, its sensitivity remains limited with nucleic acid detection being the superior standard. Laboratory-based nucleic acid detection methods, such as polymerase chain reaction (PCR) and reverse-transcriptase polymerase chain reaction (RT-PCR) have been developed and approved by the World Health Organization and the Center for Disease Control for viral pathogen detection.[2,3] However, most PCR-based methods are time-consuming and require multiple RNA/DNA extraction and purification steps prior to amplification, temperature cycling, special laboratory equipment, and trained personnel. These requirements limit the application of PCR in point-of-care (PoC) settings. Since 2020, under the pressure of the corona pandemic, several isothermal nucleic acid amplification tests (NAATs) have been authorized by the U.S. Food and Drug Administration for emergency use in the laboratory and at the PoC. These tests offer high sensitivity and specificity based on PCR-like nucleic acid detection while reducing sample preparation steps and the complexity of required equipment.[4–6] However, despite poor accuracy compared to NAATs,[7] antigen tests were the most commonly used PoC tests for SARS-CoV-2

[a] *Leibniz Institute of Polymer Research Dresden, Division Polymer Biomaterials Science, Hohe Straße 6, 01069 Dresden, Germany. E-mail: krieg@ipfdd.de, renner@ipfdd.de*
[b] *TU Dresden, Center for Regenerative Therapies Dresden, Cluster of Excellence Physics of Life, and Faculty of Chemistry and Food Chemistry, Fetscherstraße 105, 01307 Dresden, Germany*
[c] *Institute of Medical Microbiology and Virology, Faculty of Medicine, Technische Universität Dresden, Fetscherstraße 74, 01307 Dresden, Germany*
[d] *Institute for Clinical Chemistry and Laboratory Medicine, University Hospital Carl Gustav Carus, Technische Universität Dresden, Fetscherstraße 74, 01307 Dresden, Germany*
[e] *Institute for Clinical Chemistry and Laboratory Medicine, Städtisches Klinikum Dresden, Friedrichstr. 41, 01067, Dresden, Germany*
[f] *Department of Infectious Diseases, Medical Microbiology and Hygiene, Heidelberg University, Medical Faculty Heidelberg, Im Neuenheimer Feld 324, 69120 Heidelberg, Germany*
† These authors contributed equally to this work.

detection during the 2020–2023 pandemic, primarily due to their low cost, short assay time, and ease of use.[8–10] Therefore, further progress is needed to develop PoC-NAAT diagnostic platforms with higher accuracy and comparable ease of use to antigen tests.

Most PoC devices are engineered using paper, soft lithography, or 3D-printed microfluidic platforms.[11,12] Microfluidic platforms enable rapid sample processing, amplification, multiplexing, and pathogen detection in a streamlined manner while keeping the reagent costs low.[11,13–15] Isothermal NAATs have several attractive features, including the ability to detect small numbers of pathogens with high specificity at low cost, as well as the relative ease of assay set-up. The introduction of isothermal amplification has made it easier to integrate NAATs into PoC devices. Various isothermal amplification methods, such as loop-mediated amplification (LAMP),[16,17] recombinase polymerase amplification (RPA),[15,18] NASBA,[19,20] rolling circle amplification,[21,22] Cas-assisted detection,[5,23,24] riboswitches,[25,26] and transcription switches[27–29] have been developed. Among these, LAMP has been extensively investigated and adapted for commercial use in PoC settings for several viral and bacterial pathogen detection.[17,30–32] LAMP employs strand displacement polymerase and four to six target-specific primers. When used in combination with a reverse transcriptase (RT-LAMP) it can be used to rapidly detect RNA viruses with comparable clinical diagnostic accuracy to RT-PCR tests.[33,34]

Various PoC LAMP-based diagnostic platforms have recently been developed. Ganguli *et al.* developed a three-dimensional cartridge and smartphone reader LAMP PoC device for the detection of SARS-CoV-2.[35] Despite the good limit of detection (LOD) of Orf 1a (500 copies μL^{-1}), S and Orf8 (5000 copies μL^{-1}), and N (50 copies μL^{-1}) genes in a 16 μL sample volume, the cartridge design cannot be multiplexed to analyze various viral pathogens simultaneously, thus reducing the clinical applicability of the platform. Lim *et al.* developed a PoC platform for the detection of early B.1.1.7 variant strains of the SARS-CoV-2 virus.[36] This approach focused on the binary detection of the N-gene and S-gene to target regions of the virus sequence that are homologous and conserved across SARS-CoV-2. Importantly, this device demonstrated the feasibility of incorporating several variants on a single platform and the ability to differentiate between them if suitable primers are designed. However, the platform still requires a lysis step, it cannot detect multiple pathogens and requires pressure-driven flow (syringe/pumps). Most platforms rely on auxiliary devices limiting their clinical acceptance over antigen tests.[11,36] Continuous development is required to find modular, adaptable, accurate, easy-to-manufacture, and user-friendly diagnostic platforms that simultaneously eliminate the need for large laboratory-based auxiliary devices.

To avoid external application of pressure-driven flow, Soares and colleagues presented an integrated centrifugal microfluidic platform prepacked with LAMP reagents.[37] The design featured radially arranged wells preloaded with LAMP reagents. By adding the patient sample to a central inlet and rotating the platform, centrifugal force enables the distribution of the sample into these wells. Renner *et al.* developed an alternative degas-driven, self-loading polydimethylsiloxane (PDMS)-based microfluidic platform for the detection of multiple emerging bacterial pathogens.[14] The latter method provides a promising alternative to the sample-filling mechanism for multiplex assays which requires little energy and can be applied in resource-limited environments.

Here, we present a valve-free and pump-free microfluidic platform for multiplexed viral pathogen detection using LAMP, which we call *VirChip*. Our results demonstrate that *VirChip* can be used for simultaneous, sensitive, selective, rapid, and cost-effective detection of several highly relevant viral respiratory pathogens (SARS-CoV-2, influenza, and RSV), which typically cause similar clinical symptoms. *VirChip* enables the use of lower temperatures and shorter sample analysis times with comparable accuracy and sensitivity to standard laboratory tests.[10,38] Furthermore, we demonstrate clinical sample testing against multiple targets without extensive sample purification steps. Lastly, the *VirChip* design is adaptable and can include numerous targets in a single device (multiplexed), thereby increasing the versatility and diagnostic value of the chip.

Experimental methods

Materials and reagents

All primers listed in SI Table S1 were obtained from Integrated DNA Technologies (IDT, Leuven, Belgium), diluted in nuclease-free water, and stored at −20 °C. WarmStart LAMP kit (DNA&RNA, E1700S), WarmStart RTx reverse transcriptase (M0380L, 15 000 U mL^{-1}), WarmStart Bst 2.0 polymerase (M0538S, 8000 U mL^{-1}), LAMP fluorescent dye (Cat. # B1700), recombinant albumin (Cat. # B9200) and deoxynucleotide solution (dNTP, N0447S, 10.0 mM) were obtained from New England Biolabs (Ipswich, MA, USA). TaqMan Control Genomic DNA (Human, 10 ng μL^{-1}) and betaine (Cat. # J77507) were obtained from Thermo Fisher Scientific (Vilnius, Lithuania). D-(+)-trehalose dehydrate was purchased from Merck (Germany, Cat. # 90210), mineral oil from Carl Roth (Karlsruhe, Germany, Cat. # HP50.1), and EvaGreen® from Jena Bioscience (Jena, Germany, Cat. # PCR-379). All other solutions were prepared using reagent grade chemicals (Fisher Scientific, Waltham, MA), diluted with double deionized water (18.2 MΩ cm, Sartorius Arium Pro, Göttingen, Germany) to the intended concentration, and filtered using 0.2 μm membrane filter (Sartorius Arium Pro, Göttingen, Germany). Sylgard 184 elastomer kit (Dow Corning Corp., Midland, MI, USA) was used for device layer fabrication. All chemicals were used without further purification.

Microfluidic device fabrication and assembly

The overall device design is depicted in Fig. 1. The two-layer master mold was fabricated using a μMLA maskless mask aligner (Heidelberg Instruments, Germany) and previously reported photolithographic techniques.[39,40] A more detailed procedure for master mold fabrication is available in the SI (Fig. S1). PDMS mold replicas were cast using a Sylgard 184

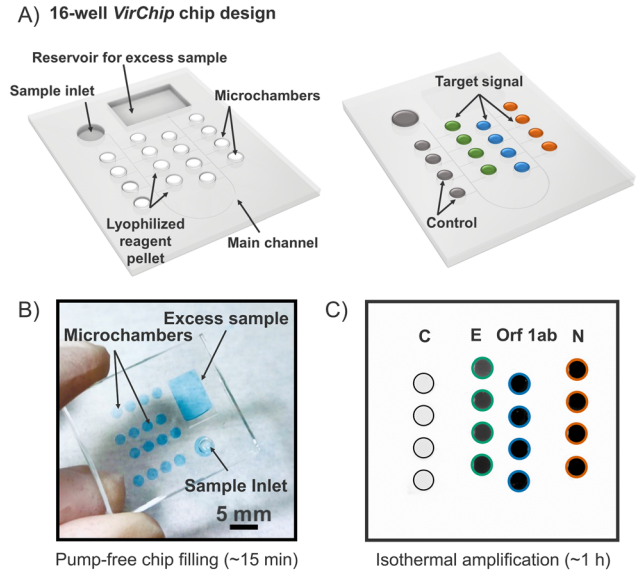

Fig. 1 (A) Schematic of *VirChip* platform (16-well) design, general operating and readout of amplified chips; (B) image of 16-well *VirChip* filled with a blue food dye solution (for demonstration only); (C) exemplary fluorescence image of a SARS-CoV-2 analysis with viral RNA isothermal amplification.

elastomer kit (10 : 1 ratio polymer base: curing agent, respectively). The sample inlet was created using a 3.0 mm diameter biopsy punch (layer 2). *VirChip* base layer (layer 1) contained 16 or 24 individual microchambers, with average volumes of 1.25 μL and 1.65 μL, respectively. All microchambers were interconnected by the main channel. Each microwell was filled with a reagent pellet (*e.g.*, primer mix, unless specified otherwise in the experimental details) and freeze-dried before sealing the top and base layers. Freeze drying of the primer mix on the base layer improves chip handling. Freeze-drying conditions are summarized in Table S2. To improve the bonding of the two layers, the top layer was placed and oxidized in a plasma cleaner (Harrick Plasma, Ithaca, NY) for 60 s.

After assembly, the PDMS microfluidic chips were de-gassed in a vacuum chamber (Harrick, Ithaca, NY) for 60 minutes. This degassing process is critical, as it enables the PDMS chips to function as micropumps, facilitating the intake of the sample and oil phase.[41] After degassing, the chips are ready for immediate use or can be stored in airtight bags for future applications. To introduce the sample into the chip, the vacuum bag is opened, and the samples are immediately loaded into the sample inlet. Alternatively, the vacuum can be released by puncturing the airtight pouch, followed by sample injection. The residual pressure differential within the chip ensures its filling within approximately 15 minutes, depending on the size of the PDMS chip and the dimensions of the channels and wells.

LAMP assay

All LAMP primer sets, and assay mixes used in this study were assembled in a PCR-UV2 cabinet (Analytik Jena, Germany). Before use, PCR-UV2 cabinet surfaces, racks, and pipettes were cleaned with 10% bleach solution and RNaseZap™ RNase decontamination solution (Invitrogen, #AM9780), followed by 70% ethanol, and a final UV treatment for 20 minutes. Assay reaction mix and *VirChip* platform assembly in the PCR UV2 cabinet reduces the probability of cross-contamination and obtaining false positive results.

RT-LAMP in reaction tubes (SARS-CoV-2). LAMP reaction mix containing a final concentration of Tris-HCl (20 mM), $(NH_4)_2SO_4$ (10 mM), KCl (50 mM), $MgSO_4$ (6 mM), Tween® 20 (0.1%), dNTP mix (1.4 mM), WarmStart Bst 2.0 polymerase (0.032 U μL^{-1}), WarmStart RTx reverse transcriptase (0.030 U μL^{-1}), betaine (10 mM), LAMP fluorescent dye (1×), and primers F3 (0.2 μM), B3 (0.2 μM), FIP (1.6 μM), BIP (1.6 μM), LF (0.4 μM) and LB (0.4 μM) was prepared in DNA LoBind tubes (Eppendorf, 0.5 mL, Cat. # 30108035). The assay mix was split into wells (9 μL per well) on a white qPCR plate (Sarstedt, # 72.1981.232), and 1 μL of sample was added to each well (final assay volume 10 μL). The qPCR plate was then immediately sealed and placed in a real-time qPCR instrument (Bio-Rad, CFX96, FAM channel) at 65 °C, and the plate was imaged every minute for 60 min.

RT-LAMP in reaction tubes (flu, RSV). To evaluate influenza (Flu A/B) and RSV (A/B) primer sets previously reported in the literature,[17,32,42,43] we used commercially available NEB assay mix and protocol given in Table S3. To test the FLU assay, the samples were FLU A (0.1 ng μL^{-1}), FLU B (0.1 ng μL^{-1}), nuclease-free water, and human genomic DNA (HGD) (10 ng μL^{-1}). To test the RSV assay, the samples were RSV A (0.1 ng μL^{-1}), RSV B (0.1 ng μL^{-1}), nuclease-free water, and HGD (10 ng μL^{-1}). After adding the samples to the assay mixes, the plates were run on a real-time qPCR instrument (Bio-Rad, CFX96, FAM channel) at 65 °C for the required time with plate reads in 1-minute cycles.

RT-LAMP on *VirChip*. LAMP-on-a-chip reaction mix containing final concentration of 20 mM Tris-HCl, 10 mM $(NH_4)_2SO_4$, 50 mM KCl, 6 mM $MgSO_4$, 0.1% Tween® 20, dNTP mix (1.4 mM), WarmStart Bst 2.0 polymerase (0.032 U μL^{-1}), WarmStart RTx reverse transcriptase (0.030 U μL^{-1}), bovine serum albumin (BSA, 0.01 μg mL^{-1}), betaine (10 mM), trehalose (7.5%), and EvaGreen (1.0 mM) were prepared in DNA LoBind tubes (Table S4).

The on-chip experiments were conducted in the following order: (i) the fully assembled microfluidic chips were de-gassed in a vacuum chamber for 60 min; (ii) meanwhile, the heat- inactivated clinical samples were collected from a −80 °C freezer and allowed to thaw at room temperature; (iii) the reaction mix was prepared in the UV cabinet. During the 20-minute UV treatment, the reagents (except enzymes and aliquoted fluorescent dye) were allowed to thaw at room temperature. The reaction mix was prepared in the UV cabinet in the order as shown in Table S4. Finally, (iv) for on-chip amplification in a 16-well chip, 6 μL RNA sample, and for a 24-well chip, a 12 μL RNA sample were added to the respective reaction mixes. After vacuum treatment of the chips, the reaction sample mix was quickly injected into the

inlet port and allowed to fill the chip for roughly 15 minutes. Then, mineral oil was pipetted onto the sample inlet, 20 μL for a 24-well chip, or 10 μL for a 16-well chip, to seal the chip and the reaction chambers. The chips were incubated on a hotplate (65 °C for 55 minutes, followed by 80 °C for 5 minutes) while covered with aluminum foil to prevent dye bleaching. Lastly, the chips were removed from the hotplate and imaged immediately using a Typhoon FLA 9500 scanner (GE), equipped with a blue laser line (excitation at 473 nm), BPB filter, 400 volts setting, and a resolution of 50 μm per pixel.

To evaluate the 24-well multiplex LAMP-on-a-chip, the chips were prefilled with the respective primer mixes and freeze-dried. For these experiments, 108 μL RT-LAMP master mix was mixed with 12 μL volume of clinical samples: heat-inactivated positive patient samples (SARS-CoV-2), RNA isolated from viral culture (FLU/RSV) or heat-inactivated negative patient sample (NTC). SARS-CoV-2 clinical samples 1–7 were used in decreasing concentrations of viral RNA (C_q range 15–21, Table S5).

Samples

To conduct preliminary sensitivity and selectivity analysis of the LAMP primers towards the DNA and RNA targets, a freshly prepared serial dilution in nuclease-free water of the N gene DNA control plasmid and *in vitro* transcribed N gene RNA was used. To evaluate the assay specificity towards different SARS-CoV-2 variants, viral RNA from lab-cultured SARS-CoV-2 B 1.1.7, B 1.177, B 1.119, B 1.258, B 1.525, and B 1.160 variants were used. The viral RNA from different variants was added to the assay mix with a final concentration of 1000 copies μL^{-1}. To evaluate the performance of the N, Orf1ab, and E gene primer sets, a target concentration of 1000 c/μL RNA (SARS-CoV-2 B.1.1.7) was used. Human genomic DNA (10 ng μL^{-1}) was used as a heat-inactivated NTC and HGD control. Nuclease-free water was used as a negative control. All relevant sample details, including RNA extraction and quantification kits, are summarized in Tables S6 and S7. The quantification of RNA samples conducted in the University Hospital Carl Gustav Carus (Dresden) is shown in the SI Table S6. The viral RNA concentration in deidentified patient samples (1–7) was predetermined using RT-PCR at the University Hospital and is summarized in Table S5.

Clinical samples. All clinical samples were stored at −80 °C in a biosafety level 3 laboratory. All clinical samples were heat-inactivated, anonymized, and analyzed using RT-PCR (exemplary calibration curves used for quantification are depicted in Fig. S3) at the University Clinic Carl Gustavus Carus prior to analysis on *VirChip*.

Data processing and statistical analysis

All fluorescence micrographs were obtained using the Typhoon FLA 9500 scanner (Sybr Green I channel). All fluorescence micrographs were processed using Fiji.[44] The results were plotted using GraphPad Prism 7 and Origin 2021 software. Fluorescence intensities used for quantification were background subtracted using control wells (wells without primers) or negative control *VirChip* (loaded with a sample without a target RNA) as a reference. Fluorescence intensity fold increase (IFI) was calculated using the following equation $\mathrm{IFI} = \frac{I_W - I_B}{I_{W0} - I_B}$ with I_W is fluorescence intensity in the target well after amplification, I_{W0} – fluorescence intensity prior to amplification in a corresponding well, and I_B – background fluorescence intensity in control chip (without RNA) or wells (without primers).

Ethical statement

All experiments were performed with anonymized leftover material from diagnostics in accordance with the Declaration of Helsinki and the institutional guidelines of Technische Universität Dresden. The study protocol was approved by the ethics committee of the Technische Universität Dresden (BO-EK-291072020).

Results

LAMP experiments in tubes

The reported SARS-CoV-2 viral loads in clinical samples range from 1 to 10^8 copies μL^{-1}, and in nasopharyngeal swabs, from 10^4 to 10^8 copies μL^{-1}.[38,45] For clinical pathogen detection, at least two regions must be targeted within the viral genome for specific identification. For SARS-CoV-2 LAMP assay development, we first tested primer sequences targeting the Orf1ab, N, and E genes. These regions have been reported to be conserved domains and low mutation rates amongst coronavirus sequences, making them promising targets for the detection of SARS-CoV-2.[42,46,47] Fig. 2A and S2 demonstrate a set of isothermal amplification curves obtained with a custom LAMP assay master mix and target-specific N, Orf1ab, and E gene primers, in a small reaction volume (10 μL). LAMP assay sensitivity comparison to the PCR is summarized in Fig. S3 and S4. The small volume was used to approximate the volume of a microfluidic well used in the study. The primer sets for the Orf1ab (blue curve), and the N gene (orange curve) demonstrated superior amplification speed. The primers for both were capable of detecting 1000 copies μL^{-1} within the first 15 min, while the E-gene (green curve) showed similar sensitivity at somewhat longer amplification times (approximately 20 min). Furthermore, we could successfully detect 100 copies μL^{-1} of RNA targeting both genes within 20 min (Fig. 2B and C). For some instances, we were able to detect ~10 copies μL^{-1} of RNA within 20 minutes (Fig. 2B and C). We observed that the detection times varied significantly at those lower RNA concentrations with primers for Orf1ab being able to perform even at very low RNA concentrations (~1–10 copies μL^{-1}). The variation in detection times for RNA concentrations can be attributed to the low reaction volume and the reduced probability of the viral RNA being present. Commercial companies circumvent this issue by performing LAMP

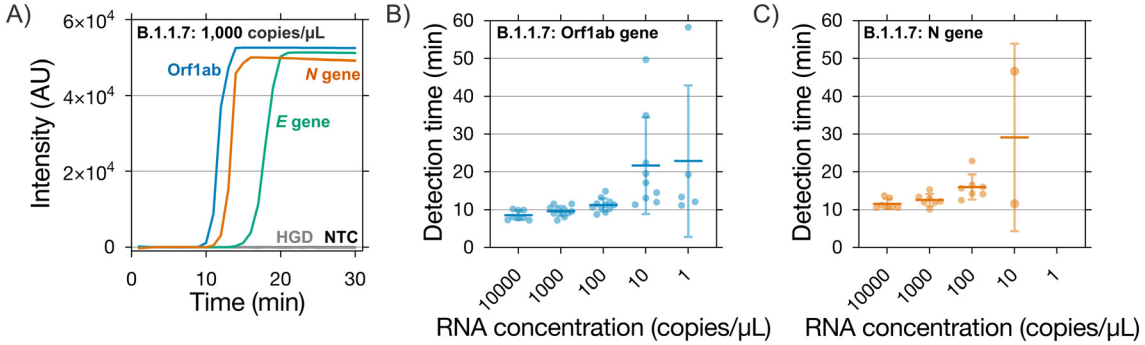

Fig. 2 Performance of different SARS-CoV-2-specific LAMP assays using viral RNA in tube reaction with reduced reaction volume. (A) LAMP assay amplification curve comparing three different primer sets targeting Orf1ab, N, and E genes of the B.1.1.7-derived RNA (1000 copies μL^{-1}) at 65 °C in a 10 µL reaction volume. (B) Sensitivity assay towards the Orf1ab gene (n = 11) and (C) sensitivity assay towards the N gene (n = 7). Data represents the compilation of results from multiple independent experiments conducted on separate days as indicated by n.

diagnostics with higher volumes, thereby increasing the cost of the diagnostic test. For example, the ID NOW assay (Abbott) uses a 200 µL reaction volume, which is 20 times larger than our LAMP tube experiment.

We then tested the SARS-CoV-2 variants B 1.1.7, B 1.177, B 1.119, B 1.258, B 1.525, and B 1.160, targeting the N gene to ensure that assay performance is not reduced by the most common viral mutations. Fig. S5 shows isothermal amplification results using purified viral RNA samples. The viral RNA concentration in these samples was 1000 copies μL^{-1}, corresponding to C_q values obtained from RT-PCR control experiments of 23 ± 0.3 cycles (Fig. S6). All tested viral samples were amplified within the first 15 minutes, and no significant differences in the amplification times were observed. These results further confirmed the suitability of the selected primers and LAMP assay for on-chip pathogen detection. On the basis of these results, we selected the N and Orf1ab genes as target genes for further assay evaluation and on-chip detection.

Clinical samples are usually collected in lytic or non-lytic viral transport mediums (VTMs), as dictated by hospital procedures. Due to this, sample pretreatment and purification often limit the capabilities of PoC assays and the streamlining of nucleic acid amplification on microfluidic platforms. Samples must first be extracted and purified prior to PCR amplification, and even minor deviations from the reaction master mix composition can lead to false negative results. In contrast, LAMP assays have shown good results in the amplification of crude samples, without the need of extensive sample pretreatment. A key advantage of LAMP is its tolerance to inhibitors. The most commonly used viral transport and storage media for clinical samples were tested to determine the maximum tolerance level for the addition of crude sample to the assay master mix. Our results demonstrate that a content of up to 10% (v/v) crude sample in eSwab (Copan) and CitoSwab (Citotest Scientific), both being non-lytic VTMs does not significantly diminish the assay performance (Fig. S7 and S8). Biocomma VTM (biocomma Limited), on the other hand, showed a notable decrease in performance at higher concentrations, and the addition of DNA/RNA collection buffer (DNA/RNA shield collection tube w/Swab, ZymoResearch) completely inhibited the amplification reaction (Fig. S7). We attributed this to the lytic nature of the respective VTMs. Clinical samples submitted for testing used in this study were therefore preserved with CitoSwab VTM at the point of sample collection. Furthermore, a 10-fold dilution would also reduce the sample viscosity, and the inhibition caused due to mucins, nucleases, and salts, ensuring assay sensitivity. It is important to note that in a PoC setting, no viral transport or storage media would be required for sample preservation, as the swabs would be processed and analyzed immediately after sample collection.

LAMP experiments in 16-well microfluidic chips

Microfluidic platforms designed for diagnostic and commercialization purposes require internal controls to be incorporated on the same chip. We designed the *VirChip* PDMS base layer with 16 wells to include triplicates of each target alongside the control wells. In this platform, each well is considered as an independent reaction chamber with a total volume of 1.25 µL. To initially compare the performance of our in-tube LAMP assay with the 16-well microfluidic platform, we first loaded three sets of four wells each with a 1.25 µL solution of master mix containing N, E, and Orf1ab primers. The four wells closest to the sample inlet were not loaded with primers and master mix and served as internal controls. The position of the control wells near the inlet reduces the risk of cross-contamination. Secondly, the PDMS base layer was freeze-dried for 6 hours, sealed, and degassed for one hour in a vacuum chamber according to the procedure described in the methods section. To stabilize the reagent pellet during drying and to reduce the adsorption of reagent to the PDMS walls, 7.5% trehalose and 0.05 µg μL^{-1} BSA were added to the master mix (SI Fig. S9).[48–50] Then, a purified SARS-CoV-2 RNA sample (100 000 copies μL^{-1}) in nuclease-free water was introduced into the microfluidic chip, followed by PCR mineral oil (10 µL) to seal each well. Finally, the 16-well chip was incubated at 65 °C, and fluorescence images were recorded at different time points for up to 60 min. Fig. 1C shows an exemplary fluorescence image of a 16-well microfluidic chip after 45 min of incubation at 65 °C. We observed a 4- to 6-fold increase in fluorescence in the

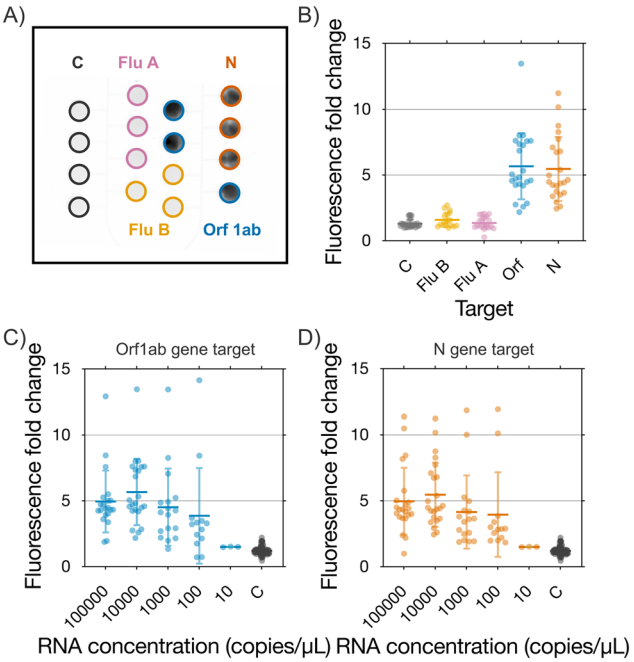

Fig. 3 Performance of the 16-well SARS-CoV-2 multiplex LAMP-on-a-chip. (A) Fluorescence image of a 16-well multiplex chip prefilled with primers specific to influenza A/B (FluA and FluB), alongside Orf1ab gene and N gene targets of SARS-CoV-2. RNA concentration 10 000 copies μL^{-1}, 65 °C, 60 min. (B) Data analysis from 16-well chips prefilled with Flu A, Flu B, Orf1ab and N gene targets subjected to 10 000 copies μL^{-1} of RNA (*C- NTC, SARS-CoV-2, Orf1ab, FLU A- influenza A, FLU B- influenza B). The chips were incubated at 65 °C for 1 hour. Each point represents the data collected from one well. Sensitivity of 16-well chips for the detection of (C) the Orf1ab and (D) the N gene targets of SARS-CoV-2 when loaded with SARS-CoV-2 RNA with different concentrations. Data represents the compilation of results from multiple independent experiments conducted on separate days as indicated by n: $n \geq 3$.

target wells for the E, Orf1ab, and N genes compared to the control wells. In particular, the N and Orf1ab wells showed an approximately 5-fold increase within 30 minutes of incubation (4.9 ± 0.2 and 4.5 ± 0.3, respectively) (Fig. 3C, D and S10). These results were in good agreement with those obtained in small reaction volumes in tubes. Furthermore, we confirmed that the interface of oil/air/water remained intact before and after incubation (Fig. S11), ensuring no crosstalk between the wells. To ensure amplification of samples with low viral loads, a 60 min incubation time was used for all further on-chip experiments. The fluorescence intensity after 60 min was used as the endpoint of the assay for quantification in subsequent experiments.

Next, we investigated the specificity of the assay for the target virus by incorporating non-specific primer sets on-chip. For this purpose, Influenza A/B primer sets were used as non-specific primers. The suitability of influenza A/B primers was confirmed by LAMP experiments in tubes as described above (Fig. S12). No cross-reactivity with SARS-CoV-2 was observed. However, on-chip, the dye (NEB, LAMP fluorescent dye, #1700S) intercalated with the primers present in the wells, leading to an increase in the fluorescence intensity in the corresponding wells. To avoid false positive results in the following experiments and to improve the signal-to-noise ratio, we investigated the suitability of other intercalating dyes for on-chip quantification. DNA intercalating dyes QuantiFluor dsDNA dye, SYTO 9, EvaGreen, and SYBR Green I have previously been used in PoC-applications with relatively good results and were therefore selected for this study.[51,52] We tested different dye concentrations to evaluate the inhibitory effects on the LAMP reaction (up to 1 μM) for the amplification of SARS-CoV-2 viral RNA (for the N gene target). SYTO 9 showed no inhibitory effects on the LAMP reaction, and EvaGreen showed minor effects with an improved signal-to-noise ratio compared to SYTO 9 (Fig. S13). On the other hand, Quant Fluor dsDNA dye and SYBR Green I showed strong inhibitory effects on the amplification (Fig. S13). For further on-chip experiments, we selected EvaGreen as the most suitable dye due to its good signal-to-noise ratio and commercial availability.

The 16-well multiplex chip was used to investigate the specificity and selectivity of the selected primers to distinguish between SARS-CoV-2 and influenza A/B. An exemplary fluorescence image of a microfluidic chip obtained after incubation at 65 °C for 60 min is shown in Fig. 3A. A similar set-up chip loaded with nuclease-free water was used as a negative control (Fig. S14). We observed an up to 13-fold increase in the fluorescence intensity in wells with the target-specific primer sets (Orf1ab and N genes, Fig. 3B). No significant fluorescence increase was detected in the wells pre-loaded with influenza A/B specific primer sets or in the control wells (no LAMP primers present) (Fig. 3B and S15). Additionally, we conducted experiments with different concentrations of SARS-CoV-2 RNA ranging from 10 to 100 000 copies μL^{-1} and analyzed the increase in fluorescence compared to the control well intensity. The data revealed that multiplex LAMP-on-a-chip is highly specific. We found that higher RNA concentration solutions (1000–100 000 copies μL^{-1}) showed on average an 4- to 13-fold increase in the target-specific wells, while lower RNA concentration solutions (100 copies μL^{-1}) resulted in a 2- to 10-fold fluorescence change (Fig. 3C and D).

LAMP experiments in 24-well microfluidic chips

To demonstrate the clinical value and adaptability of our platform, we designed and fabricated a 24-well microfluidic chip to accommodate wells for a larger number of respiratory pathogens (Fig. 4A and S1b). The 24-well chip contained a negative control (no primers) and a positive control (human β-actin, HGD), alongside three wells for each target viral pathogen: influenza A, influenza B, SARS-CoV-2, RSV A, and RSV B. We identified previously published primer sets for influenza A/B and RSV A/B. These specific primers were tested before being incorporated into the microfluidic chip. The detailed procedure for fabricating the device and the results of the primer testing in tubes are summarized in the SI.

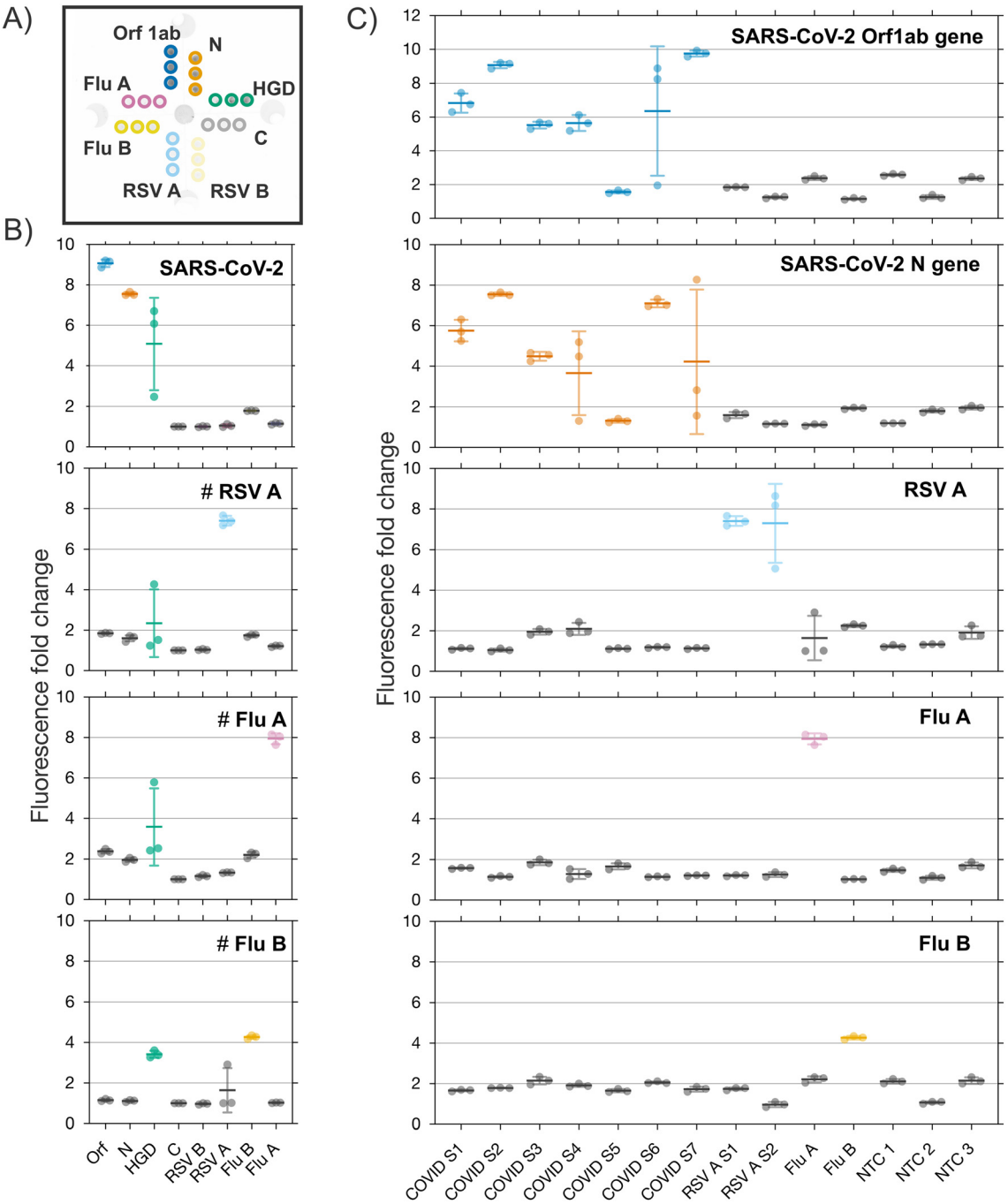

Fig. 4 Performance of the 24-well SARS-CoV-2 multiplex LAMP-on-a-chip using crude patient samples. (A) Fluorescence image of a 24-well multiplex chip prefilled with primer mixes specific to Flu A/B, RSV A/B, no primer- C, human β-actin- HGD, Orf1ab and N gene targets of SARS-CoV-2. Clinical SARS-CoV-2 sample, 65 °C, 60 min. Other fluorescence images in Fig. S19. (B) Representative data from multiplex chip experiments show the increase in fluorescence in different wells after heat-inactivated SARS-CoV-2, and spiked-in RSV A, FLU A, and FLU B samples (indicated by #) incubation on chip. n = 3. (C) Fluorescence fold increase with different clinical samples used for *VirChip* testing. The wells in color denote the wells expected to show an increase in fluorescence.

Given the use of non-lytic VTM, we also evaluated whether an additional chemical lysis step after heat-inactivation of sample could improve the sensitivity of SARS-CoV-2 detection. Hence, we performed a SARS-CoV-2 viral lysis experiment by adding tris(2-carboxyethyl)phosphine (TCEP, 10 mM) to the nasal swab VTM and incubating it for different time points (up to 30 min).[53] The experimental results showed that the addition of lysis reagent to the heat-inactivated sample is not necessary, and that the crude sample can be injected into the chip without further purification or lysis step (Fig. S18). This finding contrasts with previous reports,[54] likely due to our heat-inactivation

protocol and the use of LAMP, which operates at elevated temperatures (65 °C), potentially aiding additional viral lysis during amplification.

We used spiked-in RNA VTM samples of purified RSV A and influenza A/B (Flu A/B) to test the performance of the 24-well chip setup in identifying Influenza and RSV. The mean concentration of Influenza viral RNA in nasal swabs (clinical samples) is $\sim 10^6$ copies mL^{-1},[55] while the concentration of RSV viral load in clinical samples can vary considerably, ranging from $\sim 10^3$ to 10^{10} copies mL^{-1}.[56–58] To evaluate *VirChip* performance, we used a 0.1 ng μL^{-1} viral RNA concentration ($\sim$20 000 copies μL^{-1}) to mimic the viral load of clinical samples. Typical examples of fluorescence images obtained after chip incubation with the corresponding viral pathogen sample are shown in Fig. S16. The assay performed with samples spiked with Flu A/B and RSV RNA showed at least a fourfold increase in fluorescence for these sample wells (Fig. 4B). Furthermore, no significant increase in fluorescence was observed in the RSV B wells in the absence of RNA, confirming the specificity of the LAMP primer sets (Fig. S17). Our results indicate that the multiplex chips exhibit little or no cross-target amplification (Fig. 4C).

Finally, we tested the 24-well platform (Fig. S1b) with crude, heat-inactivated SARS-CoV-2 patient samples, and spiked-in RNA VTM samples for RSV and Flu. An exemplary fluorescence image of a 24-well chip after amplification with a patient sample is shown in Fig. 4A and S19. Analysis of the SARS-CoV-2 patient samples demonstrated an increase in fluorescence intensity in target-specific N and Orf1ab, as well as in the HGD (Fig. 4B). In both Orf1ab and N gene detection assays, on average a 4–8-fold increase in fluorescence was observed in the wells (Fig. 4B). Analysis of the collected clinical patient samples showed that the detected fluorescence fold changes in the *VirChip* corresponded fairly well with the qPCR analysis (Table S5). Quantified fluorescence fold increase from individual runs is summarized in Fig. S20. Of the samples tested, only the Covid S5 sample showed no increase in fluorescence in the corresponding wells. Visual inspection of this sample revealed a distinct color change (pale to yellow), which differed substantially from the pale appearance of other patient samples obtained from the clinic. This indicated a pH shift, which could be due to microbial contamination, improper transfer or storage of the patient sample, thereby compromising the sample's quality. Notably, all other samples performed as expected, confirming that *VirChip* reliably detects positives when the sample quality is preserved. It is expected that direct injection at the point of sample collection would limit the possibility of sample degradation or contamination during storage or transport. We further confirmed the platform using negative patient samples (no viral pathogens present), and no significant amplification was observed (Fig. S20). Altogether, *VirChip* allows for the precise detection of infected patients and to distinguish SARS-CoV-2 from RSV A and influenza A and B (Fig. 4C).

Conclusions

We have developed a new diagnostic platform, VirChip, to detect various viral pathogens at the point of care. VirChip is a multiplex LAMP-based isothermal amplification platform that can detect multiple pathogens simultaneously with good specificity and sensitivity. Proof-of-concept experiments demonstrate that VirChip can be used to analyze crude viral samples without extensive sample purification. Furthermore, the platform can be easily adapted to incorporate additional targets based on emerging clinical needs, *e.g.*, combining the detection of viral with bacterial and fungal pathogens.

Future developments steps for the field-deployable VirChip could include strategies for freeze-drying all reagents in the device by using alternative materials,[59] coatings[60] or passivation strategies to reduce reagent loss and background signal. Alternatively, lyophilized enzyme pellets could be stored in an upstream chamber that mixes with the sample upon loading, or a hybrid chip made of plastic and PDMS parts could be produced, in which critical reagents are lyophilized in a plastic insert or blister pack that interfaces with the PDMS chip.[59] We also explored sample pre-treatment strategies using TCEP as a chemical lysis reagent, which had no significant effect on the amplification of heat-inactivated COVID-19 samples. Chemical additives such as TCEP may nevertheless be beneficial in settings where nucleases are not completely inactivated by freeze–thaw cycles. Future work will optimize sample pretreatment for other pathogens and clinical sample types, and further investigate different methods of sample processing. In an ideal scenario, it might be possible to develop optimized buffers compatible with VirChip, which is a common practice amongst PoC tests. At this stage of the development, we closed the device by adding small amounts of mineral oil to avoid cross-contaminations between different pathogen wells. Being impractical in field operations, we anticipate that an air barrier will be a sufficient sealant.

We are currently working on the development of a fully integrated mobile device for multiplexed detection. The strength of our system is that it avoids costly components like pumps or valves, which in turn keep the instrument design simple. We estimated the material cost per chip to be roughly 4 USD at a small batch scale (SI Table S8). Our current benchtop setup uses a hot plate and a laboratory fluorescence imager, but we envision a more compact and low-cost integrated device for field use. For example, a simple Peltier heater combined with an LED excitation source and photodiode or camera for fluorescence detection could be engineered for real-time measurements in a portable format.[61,62] A simple integrated reader, could be produced at scale on the order of a few hundred USD (SI Table S9), and used to simultaneously read multiple *VirChip* devices at an amplification end-point. With the current setup, *VirChip* will allow for on-site (patient-visit) rapid parallel detection of viral and bacterial pathogens, as well as in emergency room settings, to dramatically reduce the detection time of currently available technologies and to quickly isolate

contagious patients. This simple, robust, and easy-to-use platform should enable a swift integration and will therefore simplify the workflow of emergency rooms.

Author contributions

Beatrise Berzina: experimental design, data analysis, manuscript writing, and editing. Krishna Gupta: experimental design, data analysis, manuscript writing. Rayan Suliman: experimental design, clinical sample analysis, and supervision; Peter Mirtschink: project supervision; Alexander Dalpke: project supervision; Carsten Werner: project supervision; Elisha Krieg: project supervision, data analysis, manuscript writing, and editing; Lars David Renner: project supervision, data analysis, manuscript writing, and editing.

Conflicts of interest

The authors declare no competing financial interest.

Data availability

Supplementary information is available. See DOI: **https://doi.org/10.1039/D5LC00509D**.

The original contributions presented in the study are included in the article/supplementary information (SI), further inquiries can be directed to the corresponding author/s.

Acknowledgements

The authors would like to thank Prof. Triantafyllos Chavakis, Leonie Wilke, MSc. Alexa Laubner, and Dr. Marlena Stadtmüller from the University Clinic Carl Gustav Carus for providing access to clinical samples and information regarding the clinical sample processing procedure at the University Clinic. This work was supported by the Else Kröner Fresenius Center for Digital Health (EKFZ). E.K. acknowledges funding by the Federal Ministry of Education and Research (BMBF) in the program *NanoMatFutur* (Grant nr. 13XP5098). L.D.R. acknowledges funding by the Volkswagen Foundation.

References

1 T. P. Peacock, L. Moncla, G. Dudas, D. VanInsberghe, K. Sukhova and J. O. Lloyd-Smith, *et al.*, The global H5N1 influenza panzootic in mammals, *Nature*, 2025, **637**, 304–313.
2 CDC Division of Viral Diseases. 2019-Novel Coronavirus (2019-nCoV) Real-Time RT-PCR Diagnostic Panel: Instructions for Use. CDC 2019-Novel Coronavirus (2019-nCoV) Real-Time RT-PCR Diagnostic Panel. 2023;16–28.
3 V. Corman, O. Landt, M. Kaiser, R. Molenkamp, A. Meijer and D. K. Chu, *et al.*, Detection of 2019 novel coronavirus (2019-nCoV) by real-time RT-PCR, *Eurosurveillance*, 2020, **25**(3), 1–8.
4 B. B. Oliveira, B. Veigas and P. V. Baptista, Isothermal Amplification of Nucleic Acids: The Race for the Next Gold Standard, *Front. Sens.*, 2021, **2**, 1–22.
5 M. J. Kellner, J. G. Koob, J. S. Gootenberg, O. O. Abudayyeh and F. Zhang, SHERLOCK: nucleic acid detection with CRISPR nucleases, *Nat. Protoc.*, 2019, **14**(10), 2986–3012.
6 R. Weissleder, H. Lee, J. Ko and M. J. Pittet, COVID-19 diagnostics in context, *Sci. Transl. Med.*, 2020, **12**(546), 1–5.
7 S. E. Smith-Jeffcoat, A. M. Mellis, C. G. Grijalva, H. K. Talbot, J. Schmitz and K. Lutrick, *et al.*, SARS-CoV-2 Viral Shedding and Rapid Antigen Test Performance — Respiratory Virus Transmission Network, November 2022–May 2023, *MMWR Morb. Mortal. Wkly. Rep.*, 2024, **73**(16), 365–371.
8 S. Katzenschlager, L. E. Brümmer, S. Schmitz, H. Tolle, K. Manten and M. Gaeddert, *et al.*, Comparing SARS-CoV-2 antigen-detection rapid diagnostic tests for COVID-19 self-testing/self-sampling with molecular and professional-use tests: a systematic review and meta-analysis, *Sci. Rep.*, 2023, **13**(1), 21913.
9 A. Soni, C. Herbert, H. Lin, Y. Yan, C. Pretz and P. Stamegna, *et al.*, and Asymptomatic SARS-CoV-2 Infection, *Ann. Intern. Med.*, 2023, **176**(7), 975–982.
10 H. Scheiblauer, A. Filomena, A. Nitsche, A. Puyskens, V. M. Corman and C. Drosten, *et al.*, Comparative sensitivity evaluation for 122 CE-marked rapid diagnostic tests for SARS-CoV-2 antigen, Germany, September 2020 to April 2021, *Eurosurveillance*, 2021, **26**(44), 1–13.
11 N. Atceken, M. Munzer Alseed, S. R. Dabbagh, A. K. Yetisen and S. Tasoglu, Point-of-Care Diagnostic Platforms for Loop-Mediated Isothermal Amplification, *Adv. Eng. Mater.*, 2023, **25**(8), 2201174.
12 Y. Manmana, T. Kubo and K. Otsuka, Recent developments of point-of-care (POC) testing platform for biomolecules, *TrAC, Trends Anal. Chem.*, 2021, **135**, 116160.
13 T. Zhang, R. Deng, Y. Wang, C. Wu, K. Zhang and C. Wang, *et al.*, A paper-based assay for the colorimetric detection of SARS-CoV-2 variants at single-nucleotide resolution, *Nat. Biomed. Eng.*, 2022, **6**(8), 957–967.
14 L. D. Renner, J. Zan, L. I. Hu, M. Martinez, P. J. Resto and A. C. Siegel, *et al.*, Detection of ESKAPE Bacterial Pathogens at the Point of Care Using Isothermal DNA-Based Assays in a Portable Degas-Actuated Microfluidic Diagnostic Assay Platform, *Appl. Environ. Microbiol.*, 2017, **83**(4), e02449-16.
15 L. Magro, B. Jacquelin, C. Escadafal, P. Garneret, A. Kwasiborski and J. C. Manuguerra, *et al.*, Paper-based RNA detection and multiplexed analysis for Ebola virus diagnostics, *Sci. Rep.*, 2017, **7**(1), 1347.
16 T. Notomi, H. Okayama, H. Masubuchi, T. Yonekawa, K. Watanabe and N. Amino, *et al.*, Loop-mediated isothermal amplification of DNA, *Nucleic Acids Res.*, 2000, **28**(12), E63.
17 I. Takayama, M. Nakauchi, H. Takahashi, K. Oba, S. Semba and A. Kaida, *et al.*, Development of real-time fluorescent reverse transcription loop-mediated isothermal amplification assay with quenching primer for influenza virus and respiratory syncytial virus, *J. Virol. Methods*, 2019, **267**, 53–58.
18 O. Piepenburg, C. H. Williams, D. L. Stemple and N. A. Armes, DNA Detection Using Recombination Proteins, *PLoS Biol.*, 2006, **4**(7), e204.

19 M. C. Keightley, P. Sillekens, W. Schippers, C. Rinaldo and K. S. George, Real-time NASBA detection of SARS-associated coronavirus and comparison with real-time reverse transcription-PCR, *J. Med. Virol.*, 2005, **77**(4), 602–608.
20 J. Compton, Nucleic acid sequence-based amplification, *Nature*, 1991, **350**, 91–92.
21 H. N. Lee, J. Lee, Y. K. Kang, J. H. Lee, S. Yang and H. J. Chung, A Lateral Flow Assay for Nucleic Acid Detection Based on Rolling Circle Amplification Using Capture Ligand-Modified Oligonucleotides, *BioChip J.*, 2022, **16**(4), 441–450.
22 A. Fire and S. Q. Xu, Rolling replication of short DNA circles, *Proc. Natl. Acad. Sci. U. S. A.*, 1995, **92**(10), 4641–4645.
23 M. Azhar, R. Phutela, M. Kumar, A. H. Ansari, R. Rauthan and S. Gulati, *et al.*, Rapid and accurate nucleobase detection using FnCas9 and its application in COVID-19 diagnosis, *Biosens. Bioelectron.*, 2021, **183**, 113207.
24 Y. Sun, L. Yu, C. Liu, S. Ye, W. Chen and D. Li, *et al.*, One-tube SARS-CoV-2 detection platform based on RT-RPA and CRISPR/Cas12a, *J. Transl. Med.*, 2021, **19**(1), 74.
25 D. Ma, L. Shen, K. Wu, C. W. Diehnelt and A. A. Green, Low-cost detection of norovirus using paper-based cell-free systems and synbody-based viral enrichment, *Synth. Biol.*, 2018, **3**(1), ysy018.
26 A. A. Green, P. A. Silver, J. J. Collins and P. Yin, Toehold switches: de-novo-designed regulators of gene expression, *Cell*, 2014, **159**(4), 925–939.
27 J. K. Jung, K. K. Alam, M. S. Verosloff, D. A. Capdevila, M. Desmau and P. R. Clauer, *et al.*, Cell-free biosensors for rapid detection of water contaminants, *Nat. Biotechnol.*, 2020, **38**(12), 1451–1459.
28 A. Patino Diaz, S. Bracaglia, S. Ranallo, T. Patino, A. Porchetta and F. Ricci, Programmable Cell-Free Transcriptional Switches for Antibody Detection, *J. Am. Chem. Soc.*, 2022, **144**(13), 5820–5826.
29 K. Gupta and E. Krieg, Y-switch: a spring-loaded synthetic gene switch for robust DNA/RNA signal amplification and detection, *Nucleic Acids Res.*, 2024, **52**(17), e80–e80.
30 Y. Dong, Y. Zhao, S. Li, Z. Wan, R. Lu and X. Yang, *et al.*, Multiplex, Real-Time, Point-of-care RT-LAMP for SARS-CoV-2 Detection Using the HFman Probe, *ACS Sens.*, 2022, **7**(3), 730–739.
31 M. Dou, N. Macias, F. Shen, J. D. Bard, D. C. Domínguez and X. Li, Rapid and Accurate Diagnosis of the Respiratory Disease Pertussis on a Point-of-Care Biochip, *EClinicalMedicine*, 2019, **8**, 72–77.
32 L. L. M. Poon, C. S. W. Leung, K. H. Chan, J. H. C. Lee, K. Y. Yuen and Y. Guan, *et al.*, Detection of Human Influenza A Viruses by Loop-Mediated Isothermal Amplification, *J. Clin. Microbiol.*, 2005, **43**(1), 427–430.
33 Q. Song, X. Sun, Z. Dai, Y. Gao, X. Gong and B. Zhou, *et al.*, Point-of-care testing detection methods for COVID-19, *Lab Chip*, 2021, **21**(9), 1634–1660.
34 R. Lu, X. Wu, Z. Wan, Y. Li, X. Jin and C. Zhang, A Novel Reverse Transcription Loop-Mediated Isothermal Amplification Method for Rapid Detection of SARS-CoV-2, *Int. J. Mol. Sci.*, 2020, **21**(8), 2826.
35 A. Ganguli, A. Mostafa, J. Berger, M. Y. Aydin, F. Sun and S. A. S. de Ramirez, *et al.*, Rapid isothermal amplification and portable detection system for SARS-CoV-2, *Proc. Natl. Acad. Sci. U. S. A.*, 2020, **117**(37), 22727–22735.
36 J. Lim, R. Stavins, V. Kindratenko, J. Baek, L. Wang and K. White, *et al.*, Microfluidic point-of-care device for detection of early strains and B.1.1.7 variant of SARS-CoV-2 virus, *Lab Chip*, 2022, **22**(7), 1297–1309.
37 R. R. G. Soares, A. S. Akhtar, I. F. Pinto, N. Lapins, D. Barrett and G. Sandh, *et al.*, Sample-to-answer COVID-19 nucleic acid testing using a low-cost centrifugal microfluidic platform with bead-based signal enhancement and smartphone read-out, *Lab Chip*, 2021, **21**(15), 2932–2944.
38 E. S. Savela, A. V. Winnett, A. E. Romano, M. K. Porter, N. Shelby and R. Akana, *et al.*, Quantitative SARS-CoV-2 Viral-Load Curves in Paired Saliva Samples and Nasal Swabs Inform Appropriate Respiratory Sampling Site and Analytical Test Sensitivity Required for Earliest Viral Detection, *J. Clin. Microbiol.*, 2022, **60**(2), 1–12.
39 G. G. Morbioli, N. C. Speller and A. M. Stockton, A practical guide to rapid-prototyping of PDMS-based microfluidic devices: A tutorial, *Anal. Chim. Acta*, 2020, **1135**, 150–174.
40 Y. Xia and G. M. Whitesides, Soft lithography, *Annu. Rev. Mater. Sci.*, 1998, **28**(1), 153–184.
41 N. J. Cira, J. Y. Ho, M. E. Dueck and D. B. Weibel, A self-loading microfluidic device for determining the minimum inhibitory concentration of antibiotics, *Lab Chip*, 2012, **12**(6), 1052–1059.
42 Y. Zhang, G. Ren, J. Buss, A. J. Barry, G. C. Patton and N. A. Tanner, Enhancing colorimetric loop-mediated isothermal amplification speed and sensitivity with guanidine chloride, *BioTechniques*, 2020, **69**(3), 178–185.
43 M. Jang, S. Kim, J. Song and S. Kim, Rapid and simple detection of influenza virus via isothermal amplification lateral flow assay, *Anal. Bioanal. Chem.*, 2022, **414**(16), 4685–4696.
44 J. Schindelin, I. Arganda-Carreras, E. Frise, V. Kaynig, M. Longair and T. Pietzsch, *et al.*, Fiji: an open-source platform for biological-image analysis, *Nat. Methods*, 2012, **9**, 676.
45 O. Puhach, B. Meyer and I. Eckerle, SARS-CoV-2 viral load and shedding kinetics, *Nat. Rev. Microbiol.*, 2023, **21**(3), 147–161.
46 A. Ganguli, A. Mostafa, J. Berger, M. Y. Aydin, F. Sun and S. A. Stewart de Ramirez, *et al.*, Rapid isothermal amplification and portable detection system for SARS-CoV-2, *Proc. Natl. Acad. Sci. U. S. A.*, 2020, **117**(37), 22727–22735.
47 W. E. Huang, B. Lim, C. C. Hsu, D. Xiong, W. Wu and Y. Yu, *et al.*, RT-LAMP for rapid diagnosis of coronavirus SARS-CoV-2, *Microb. Biotechnol.*, 2020, **13**(4), 950–961.
48 C. Carter, K. Akrami, D. Hall, D. Smith and E. Aronoff-Spencer, Lyophilized visually readable loop-mediated isothermal reverse transcriptase nucleic acid amplification test for detection Ebola Zaire RNA, *J. Virol. Methods*, 2017, **244**, 32–38.
49 K. Hayashida, K. Kajino, L. Hachaambwa, B. Namangala and C. Sugimoto, Direct Blood Dry LAMP: A Rapid, Stable, and Easy Diagnostic Tool for Human African Trypanosomiasis, *PLoS Neglected Trop. Dis.*, 2015, **9**(3), 1–14.

50 S. Kumar, R. Gallagher, J. Bishop, E. Kline, J. Buser and L. Lafleur, *et al.*, Long-term dry storage of enzyme-based reagents for isothermal nucleic acid amplification in a porous matrix for use in point-of-care diagnostic devices, *Analyst*, 2020, **145**(21), 6875–6886.
51 T. L. Quyen, T. A. Ngo, D. D. Bang, M. Madsen and A. Wolff, Classification of Multiple DNA Dyes Based on Inhibition Effects on Real-Time Loop-Mediated Isothermal Amplification (LAMP): Prospect for Point of Care Setting, *Front. Microbiol.*, 2019, **10**, 1–12.
52 G. Seyrig, R. D. Stedtfeld, D. M. Tourlousse, F. Ahmad, K. Towery and A. M. Cupples, *et al.*, Selection of fluorescent DNA dyes for real-time LAMP with portable and simple optics, *J. Microbiol. Methods*, 2015, **119**, 223–227.
53 B. A. Rabe and C. Cepko, SARS-CoV-2 detection using isothermal amplification and a rapid, inexpensive protocol for sample inactivation and purification, *Proc. Natl. Acad. Sci. U. S. A.*, 2020, **117**(39), 24450–24458.
54 J. Arizti-Sanz, C. A. Freije, A. C. Stanton, B. A. Petros, C. K. Boehm and S. Siddiqui, *et al.*, Streamlined inactivation, amplification, and Cas13-based detection of SARS-CoV-2, *Nat. Commun.*, 2020, **11**(1), 5921.
55 F. R. Cui, J. Wang, S. M. Opal and A. Tripathi, Isolating influenza RNA from clinical samples using microfluidic oil-water interfaces, *PLoS One*, 2016, **11**(2), 1–9.
56 L. A. H. Do, H. R. van Doorn, J. E. Bryant, M. N. Nghiem, V. C. Nguyen Van and C. K. Vo, *et al.*, A sensitive real-time PCR for detection and subgrouping of human respiratory syncytial virus, *J. Virol. Methods*, 2012, **179**(1), 250–255.
57 J. P. McGinley, G. L. Lin, D. Öner, T. Golubchik, D. O'Connor and M. D. Snape, *et al.*, Clinical and Viral Factors Associated With Disease Severity and Subsequent Wheezing in Infants With Respiratory Syncytial Virus Infection, *J. Infect. Dis.*, 2022, **226**(1), S45–S54.
58 C. M. El Saleeby, A. J. Bush, L. M. Harrison, J. A. Aitken and J. P. Devincenzo, Respiratory syncytial virus load, viral dynamics, and disease severity in previously healthy naturally infected children, *J. Infect. Dis.*, 2011, **204**(7), 996–1002.
59 N. Mytzka, S. Arbaciauskaite, N. Sandetskaya, K. Mattern and D. Kuhlmeier, A fully integrated duplex RT-LAMP device for the detection of viral infections, *Biomed. Microdevices*, 2023, **25**(4), 36.
60 H. Sasaki, H. Onoe, T. Osaki, R. Kawano and S. Takeuchi, Parylene-coating in PDMS microfluidic channels prevents the absorption of fluorescent dyes, *Sens. Actuators, B*, 2010, **150**(1), 478–482.
61 W. Chen, H. Yu, F. Sun, A. Ornob, R. Brisbin and A. Ganguli, *et al.*, Mobile Platform for Multiplexed Detection and Differentiation of Disease-Specific Nucleic Acid Sequences, Using Microfluidic Loop-Mediated Isothermal Amplification and Smartphone Detection, *Anal. Chem.*, 2017, **89**(21), 11219–11226.
62 A. M. Jankelow, H. Lee, W. Wang, T. H. Hoang, A. Bacon and F. Sun, *et al.*, Smartphone clip-on instrument and microfluidic processor for rapid sample-to-answer detection of Zika virus in whole blood using spatial RT-LAMP, *Analyst*, 2022, **147**(17), 3838–3853.

